Solution of problems of the temperature monitoring of the Earth's surface from space on the basis of the RTM method

S.V. Afonin,[1,2] V.V. Belov,[1,2] and D.V. Solomatov[1]

[1]V.E. Zuev Institute of Atmospheric Optics,
Siberian Branch of the Russian Academy of Sciences, Tomsk
[2]Tomsk State University

We consider the physical aspects of application of the RTM method for solution of the problem of the temperature monitoring of the underlying surface from space; quantitative estimates of the RTM method efficiency for detection of high-temperature objects are obtained.

Introduction

It is well known that the remote sensing of the land surface temperature (LST) from space provides for important information on many physical, chemical, and biologic processes on the Earth. For most applied problems, this information must be accurate to within 0.5–1 K. As a complement to these problems, a quite urgent problem of the fast detection and monitoring of emergency situations, namely, fires, volcanoes, earthquakes, etc., may be considered.

In recent 25 years, of concern has been active development of satellite methods of LST retrieval,[1–8] which general name is *"split-window methods"* (SW methods). As a part of this approach, the IR measurements in two spectral channels of a "split" atmospheric transparency widow of 10–13 μm are used and the well-known method of differential absorption is implemented to account for the distorting water vapor effect.

The general form of the algorithms is based on the linear relations between LST (T_S) and satellite measurements (radiation temperatures) in two spectral channels near 11 and 12 μm (T_{11} and T_{12}):

$$T_S = C + \alpha T_{11} + \beta(T_{11} - T_{12}), \qquad (1)$$

where the coefficients C, α, and β are determined on the basis of the joint statistical processing of ground- and satellite-based measurements or results of simulation of LST satellite measurements for a wide set of the meteorological models of the atmosphere.

More sophisticated form of formula (1) involves emittances ε_{11} and ε_{12} of the underlying surface for these channels, their difference $\Delta\varepsilon$, the dependence of coefficients on the moisture content, near-ground air temperature, and viewing zenith angle. This can be exemplified by the standard algorithm of remote LST measurements with the use of MODIS data.[6,7]

From the practical viewpoint, these algorithms are very simple and efficient for global LST monitoring.

However, their users cannot disregard a number of serious practical limitations:

1. The LST retrieval error (δT_S) strongly depends on errors of δT_λ measurements. For instance, it is reported[7] that $\delta T_S \approx 6.19 \delta T_\lambda$. For NOAA/AVHRR instrument, $\delta T_\lambda \approx 0.12$ K, i.e., $\delta T_S \approx 0.7$ K; while for EOS/MODIS system, $\delta T_\lambda \approx 0.05 \div 0.07$ K, i.e., $\delta T_S \approx 0.3 \div 0.4$ K.

2. The surface emittances ε_{11} and ε_{12}, as well as their difference $\Delta\varepsilon$ should be well known. It is underlined in Refs. 2 and 3 that at $\delta T_S \approx 0.5$ K the relative error $\delta\varepsilon$ of ε specification should be no more than about $0.5 \div 1\%$, and for $\Delta\varepsilon$ no worse than $0.25 \div 0.5\%$.

3. The coefficients of the algorithms are determined only for a given range of "standard" situations in the clear-sky atmosphere.

4. The algorithms take into account the thermal absorption by the water vapor; at the same time, the distortions, caused by aerosol and cirrus clouds, are ignored.

Thus, the standard LST retrieval algorithms, used in practice, do not provide for confident and universal solution of the problem of atmospheric correction of IR measurements, especially under complex (non-standard) observational conditions.

Another, more correct approach is in the use of thermal radiative transfer models. The RTM method accounts for the distorting characteristics of the atmosphere with the use of widely known computer programs of the type of LOWTRAN-7, MODTRAN, 6S, ATCOR, etc., on the basis of the *a priori* optical-meteorological information on the atmospheric state at the moment of satellite observations. Examples of the use of this approach are atmospheric corrections of radiometric data of MSU-SK, NOAA/AVHRR, Landsat, and ASTER.[9–12]

Undoubtedly, this approach offers the universality and explicit accounting for all distorting factors in solution of the problem of LST retrieval from space,

though its practical implementation requires invoking a large amount of real-time *a priori* information of the required quality and high-speed calculations.

The intensive development of computation methods and modern technologies of parallel computer programming[13,14] eliminates labor consumptions of enormous computations. Moreover, a combined approach was suggested[12]: the fast SW method for standard situations and the RTM method for situations beyond the standard limits (in the presence of aerosol and semitransparent or cirrus clouds). The software package is also described in the same work, allowing a user, by means of accessible facilities (IMAPP and MODTRAN) and on the basis of EOS/MODIS satellite information, to employ the RTM method for the complex temperature monitoring of the Earth's surface, including LST retrieval and monitoring of high-temperature objects (HTO), i.e., fires and industrial thermal sources.

This paper analyzes different aspects of application of the RTM method with the use of EOS/MODIS IR channels (20, 21/22, 31, 32) of the Earth's surface temperature monitoring and presents quantitative estimates of the RTM efficiency (as compared with standard approach) for HTO detection.

1. Distortions of thermal radiation by molecular atmosphere

It is well known that main factors of the molecular distortion of thermal radiation in EOS/MODIS channels include: the selective absorption by spectral lines of atmospheric gases and continuum absorption by line wings of H_2O and N_2. Though estimates of the influence of these factors on characteristics of upward fluxes of thermal radiation are available in the literature, the permanent development of thermal radiative transfer models necessitates some improvement of these estimates for a tighter relevance to the problems of the land surface temperature retrieval.

We used for these purposes the well-known software package LBLRTM_v11.3 (11/2007),[15] built upon the spectral line database HITRAN-2004[16] (including all changes made to January 1, 2007) and molecular continuum models MT_CKD_2.1 [Ref. 17].

1.1. Selective absorption by spectral lines of atmospheric gases

The analysis of the HITRAN-2004 data on the total intensity of the molecular spectral lines and integrated gas content W_{GAS} allows one to separate out from the total list consisting of 39 molecules the optically active molecules (in the considered EOS/MODIS spectral channels), which determine the required accuracy of the LST retrieval by the RTM method: H_2O, CO_2, O_3, N_2O, and CH_4. The figure presents the absorption functions of thermal radiation, calculated with the use of LBLRTM_v11.3 in the considered EOS/MODIS channels.
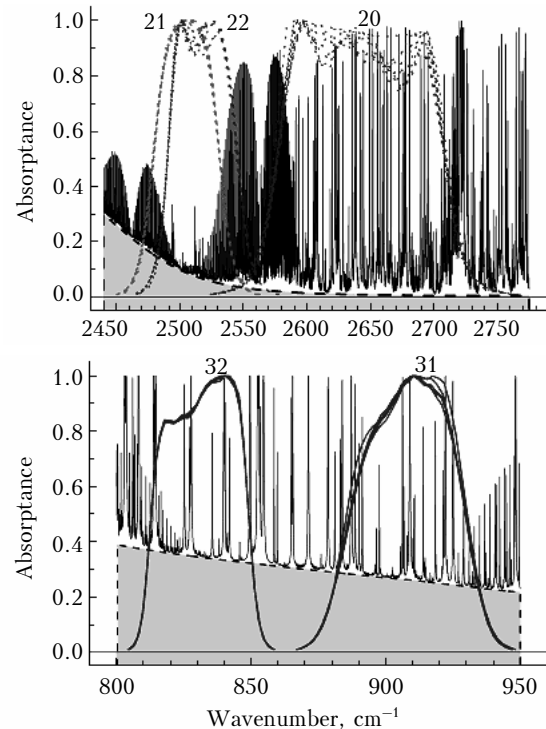

Fig. Absorption of thermal radiation in 20, 21/22, 31, and 32 EOS/MODIS spectral channels. Midlatitude summer. Shade of grey shows continuum; peaks are for lines + continuum.

The influence of the selective absorption by each molecule (and their sum) on the accuracy of the RTM method can be estimated quantitatively by calculating the change of the radiation (brightness) temperature, measured in satellite channels, provided the chosen molecule is not taken into account in the line-by-line (*LBL*) calculations. Thus, it is necessary to determine the difference

$$\delta T_\lambda(\text{mol}) = T_\lambda(\Sigma) - T_\lambda(\Sigma-\text{mol}), \qquad (2)$$

where $T_\lambda(\Sigma)$ and $T_\lambda(\Sigma-\text{mol})$ are calculated radiation temperatures, for which either all absorbing components (Σ) are taken into account or the chosen molecule ($\Sigma-\text{mol}$) is not taken into account.

Table 1 presents the δT_λ, estimates, allowing us to draw certain conclusions.

1) First of all, obviously, the influence of the selective absorption by atmospheric gases in all EOS/MODIS channels exceeds the 0.25 K level and, hence, should be accounted for within the RTM method.

2) In channels 20 and 21, the distorting effect of the selective absorption is determined by lines of H_2O, N_2O, and CH_4 molecules.

3) In channels 31 and 32, it is sufficient to take into account only the contribution of H_2O lines, with much less accounting for the CO_2 line contribution.

Thus, in the framework of the RTM method, the problem of fast specification of the confident *a priori* information concerns only the temperature and humidity profiles.

One more important condition of the successful use of the RTM method in practice is a good accuracy and high speed of calculation of selective absorption coefficients in the processing of large-volume satellite information. Obviously, the direct use of the *LBL* methods in the framework of the RTM method is impossible in view of their laboriousness; therefore, it is advisable to use simplified radiative transfer models, tested in practice and accessible to wide user community, such as the commonly known MODTRAN program. Presently, the program MODTRAN_v4.x [Ref. 19] is a commercially available product; however, its predecessor MODTRAN_v3.x [Ref. 18] and its codes are accessible (that is important) to users. Table 1 presents δT_λ(mol) calculations with the use of MODTRAN_v3.5 program, based on parameters of spectral lines from HITRAN-96 [Ref. 20] and models of molecular continuum CKD_v2.1_rev.3.3.[21] The comparison of δT_λ(mol) values, obtained by MODTRAN_v3.5 and LBLRTM_v11.3, suggests that these data disagree by less than 0.15 K, reasonably well meeting the practical accuracy requirements to the satellite-borne LST retrieval.

1.2. Continuum absorption by spectral line wings of atmospheric gases

According to the MT_CKD_v2.1 model, in addition to the selective absorption of the thermal radiation by lines, located inside the spectral channels, a marked influence is exerted by the continuum absorption by line wings of intense H_2O, CO_2, O_3, and N_2 bands, lying outside these spectral channels (see the figure). The atmospheric transparency window 3.5—4 μm is characterized by a weak H_2O continuum,

while at wavenumbers $\nu < 2600$ cm^{-1} there is a stronger N_2 continuum. In a transparency window of 10—13 μm, a strong H_2O continuum is dominated, with a simultaneous presence of a weak CO_2 continuum. The H_2O continuum is presented by two components, corresponding to self-broadening of lines (H_2O—H_2O) and air-caused line broadening (H_2O—AIR).

To quantitatively estimate the influence of each continuum component, we calculated δT_λ(cont) by analogy with δT_λ(mol) calculations:

$$\delta T_\lambda(\text{cont}) = T_\lambda(\textstyle\sum) - T_\lambda(\textstyle\sum-\text{cont}), \qquad (3)$$

where $T_\lambda(\sum)$ and $T_\lambda(\sum-\text{cont})$ are the calculated radiation temperatures, for which all absorbing components ($\sum$) are taken into account or the chosen continuum component ($\sum-\text{cont}$) is not accounted for.

Table 2 presents the δT_λ(cont) calculations, whose analysis allows us to make the following conclusions.

1) The effect of H_2O and CO_2 continuums on the radiation temperature in channels 20 and 21 is less than 0.05 K. The effect of N_2 continuum in channel 20 has the same order of magnitude; however, it markedly increases in channel 21, exceeding a level of 1 K.

2) The component H_2O—H_2O (≈ 1—2 K) dominates in channels 31 and 32, at a much less (than 0.2 K) influence of the component H_2O—AIR. The effect of CO_2 continuum is almost insignificant (less than 0.01 K).

3) Comparing the δT_λ(cont) values, obtained via LBLRTM_v11.3 and MODTRAN_v3.5 programs, we see that they disagree in channels 20, 31, and 32 by less than 0.1 K, and they increase up to 0.2 K due to N_2 continuum only in channel 21.

Table 1. Optical depth τ of atmospheric gases and distortion of radiation temperature δT_λ (mol), K. Midlatitude summer

Molecule	Spectral channel							
	20		21		31		32	
	τ	δT_λ	τ	δT_λ	τ	δT_λ	τ	δT_λ
LBLRTM_v11.3 data								
H_2O	0.1267	0.935	0.0035	0.020	0.0859	0.685	0.0827	0.662
CO_2	0.0013	0.022	0.0017	0.027	0.0027	0.034	0.0049	0.070
O_3							0.0003	0.015
N_2O	0.0175	0.319	0.0174	0.260				
CH_4	0.0102	0.145	0.0045	0.067				
Other							0.0007	0.015
All	0.1572	1.420	0.0273	0.376	0.0915	0.857	0.0889	0.765
All (*tropics*)	0.1949	1.923	0.0298	0.436	0.1209	1.151	0.1155	0.994
MODTRAN_v3.5 data								
H_2O	0.1288	0.926	0.0040	0.022	0.0756	0.615	0.0911	0.772
All	0.1584	1.416	0.0315	0.429	0.0876	0.969	0.0979	0.896
All (*tropics*)	0.1969	1.917	0.0342	0.496	0.1126	1.231	0.1239	1.119

**Table 2. Optical depth τ of molecular continuum and distortion
of radiation temperature δT_λ (cont), K. Midlatitude summer**

Component	Spectral channel							
	20		21		31		32	
	τ	δT_λ	τ	δT_λ	τ	δT_λ	τ	δT_λ
LBLRTM_v11.3 data								
H_2O-H_2O	0.0019	0.008	0.0029	0.013	0.2959	1.400	0.3956	1.825
H_2O-AIR	0.0026	0.014	0.0001	0.000	0.0112	0.072	0.0278	0.174
CO_2	0.0003	0.003	0.0034	0.041	0.0001	0.002	0.0003	0.006
N_2	0.0058	0.067	0.1052	1.251				
All	0.0106	0.093	0.1115	1.309	0.3072	1.483	0.4237	2.032
All (*tropics*)	0.0131	0.119	0.1135	1.454	0.5525	3.064	0.7558	4.060
MODTRAN_v3.5 data								
H_2O-H_2O	0.0044	0.020	0.0061	0.027	0.3188	1.491	0.4390	1.986
H_2O-AIR	0.0034	0.018	0.0002	0.001	0.0008	0.005	0.0049	0.030
N_2	0.0074	0.093	0.1174	1.445				
All	0.0152	0.131	0.1236	1.475	0.3196	1.497	0.4439	2.022
All (*tropics*)	0.0199	0.173	0.1278	1.647	0.5849	3.170	0.8099	4.144

1.3. The influence of errors in setting profiles of meteorological parameters

To date, the current databases of spectral line parameters, molecular continuum models, and thermal radiative transfer models, overall, ensure a high accuracy of accounting for the distorting influence of the atmosphere, when using the *a priori* valid information on key meteorological parameters of the atmosphere $X(z)$, where z is the height. Since the vertical profiles of $X(z)$ contain measurement (retrieval) errors $\delta X(z)$, it seems reasonable to estimate the effect of these errors on the accuracy of the RTM method.

The estimates were made as follows: 1) for the chosen profile of atmospheric meteorological parameters (e.g., meteorological model of the midlatitude summer), we calculated the radiation temperature $T_\lambda(0)$; 2) some changes $\delta X(z)$ were introduced in a given profile and the value of $T_\lambda(\delta X)$ was calculated for the distorted profile; and 3) the difference $\delta T_\lambda(\delta X) = T_\lambda(0) - T_\lambda(\delta X)$ was calculated, being the measure of the influence of the inaccuracy in setting meteorological parameters on the radiation temperature.

Table 3 presents the calculations of $\delta T_\lambda(\delta X)$ for the air temperature and moisture content, as well as the content of other atmospheric gases. For the air temperature and moisture content we have chosen $\delta T_{AIR} = +2$ K and $\delta W_{H_2O} = +20\%$ at all atmospheric levels. They can be considered as characteristic retrieval errors of atmospheric meteorologic parameters according to EOS/MODIS data.[22] For profiles of other atmospheric gases, we have chosen $\delta W_{GAS} = +40\%$ as a certain limiting value. Thus, the data of Table 3, overall, reflect the maximal effect of meteorological parameter profile errors on T_λ. Accounting for the limiting character of these estimates, we can make the following conclusions.

**Table 3. Change of radiation temperature caused by
variations of the profiles of meteorologic parameters: the
air temperature δT_{AIR}, the humidity δW_{H_2O}, and the minor
atmospheric gas content δW_{GAS}. LBLRTM_v11.3 data**

Parameter	Spectral channel			
	20	21	31	32
Midlatitude summer				
$\delta T_{AIR} = +2$ K	+0.206	+0.150	+0.632	+0.786
$\delta W_{H_2O} = +20\%$	−0.153	−0.010	−0.659	−0.820
$\delta W_{GAS} = +40\%$	−0.168	−0.151	−0.068	−0.043
Tropics				
$\delta T_{AIR} = +2$ K	+0.241	+0.147	+0.968	+1.170
$\delta W_{H_2O} = +20\%$	−0.218	−0.020	−1.199	−1.418
$\delta W_{GAS} = +40\%$	−0.186	−0.169	−0.075	−0.043

1) In channels 20 and 21, the influence of variations of profiles of all meteorologic parameters in absolute value is less than 0.25 K, which, in principle, permits one in practice to optimize the volume of calculations of the distorting atmospheric parameters.

2) In channels 31 and 32, the value of δT_λ for a given δW_{GAS} does not exceed 0.1 K; therefore, the setting of *a priori* information on the atmospheric content of minor gas constituents in these channels does not require a high accuracy. At the same time, the effect of uncertain setting of the temperature and air humidity profiles is significant ($\delta T_\lambda > 0.5$ K) for the correct treatment of the molecular distortion of the thermal radiation in the framework of the RTM method. Note that the absolute value of δT_λ is determined by the degree of the thermal radiation absorption in the channel; therefore, $|\delta T_\lambda|$ is less in channel 31 than in 32. This circumstance can be used to compensate for the effect of imperfect setting of meteorological parameters in the RTM method.

3) Note that identical signs of δT_{AIR} and δW_{H_2O} correspond to differently signed δT_λ values. That is, in

the presence of the positive correlation between δT_{AIR} and δW_{H_2O}, this circumstance may lead to mutual error compensation in setting meteorological parameters, which are key ones to the atmospheric correction. Thus, the atmospheric correction of remote IR measurements of LST becomes possible on the basis of the meteorological information with relatively low accuracy characteristics.

The latter two conclusions should be complemented with some important comments. First, the analysis of the satellite methods of the temperature and humidity profiles retrieval[22] allows us to suppose with a high degree of confidence that errors in the retrieval of the temperature and humidity have just a positive correlation. Second, the difference between $\delta T_\lambda(\delta X)$ values in channels 31 and 32 allows us to propose the compensation for the δX effect through application of the RTM method by the *"split-window"* principle, that is, the LST is to be determined as follows:

$$T_S = T_{S,31} - \Delta T_S; \; \Delta T_S = C_{ERR}(T_{S,32} - T_{S,31}), \quad (4)$$

where $T_{S,31}$ and $T_{S,32}$ are LST values, retrieved in 31 and 32 channels; $C_{ERR} \approx 2.0$ is the coefficient obtained from simulation calculations. This will ensure the RTM method resistance to uncertainties in setting the *a priori* meteorological information.

2. Application of the RTM method to detection of high-temperature objects

The RTM method was tested using data of 97 files (granules) of the telemetric information from EOS/MODIS (Terra satellite, daytime images) for June 2006, pertaining to the West Siberian territory. As test objects for observations, we have chosen 13 torches from combustion of accompanying gas in oil-gas fields of Tomsk and southern Tyumen Regions.

The choice of torches was determined by their stability and availability of their geographic coordinates, necessary for the torch identification. Thus, the torches were a set of varying-intensity thermal objects, allowing the effective elaboration of the methods of satellite-based HTO detection under different conditions of satellite observations.

For elaboration of satellite methods, we used two variants of the standard algorithm MOD14_v5.0.1,[23] as well as the RTM methods with the use of our methodical innovations and software.[12]

2.1. MOD14 algorithm

After the cloud- and water-covered pixels are identified, the potential fires are determined with the use of three conditions:

$$1) \; T_{21} > 310 \text{ K}; \; 2) \; \Delta T > 10 \text{ K}; \; 3) \; \rho_{0.86} < 0.3, \quad (5)$$

where T_{21} and T_{31} are radiation temperatures in channels 21/22 and 31 of the EOS/MODIS sensor;

$\rho_{0.86}$ is the reflectance in channel 2 of this sensor; and $\Delta T = T_{21} - T_{31}$.

Then, for background pixels, adjacent to the potential fires, the following statistical characteristics are determined: mean values (T_{21}^*, T_{31}^*, ΔT^*) and mean absolute deviations (μ_{21}, μ_{31}, $\mu_{\Delta T}$) for T_{21}, T_{31}, and ΔT, respectively.

Further, the pixels, flagged as potential fires, are examined through the series of tests:

Test 1. $T_{21} > 360$ K (320 K for nighttime pixels).

$$\textit{Test 2. } \Delta T > \Delta T^* + C_1\mu_{\Delta T}.$$
$$\textit{Test 3. } \Delta T > \Delta T^* + C_2. \quad (6)$$
$$\textit{Test 4. } T_{21} > T_{21}^* + C_3\mu_{21}.$$
$$\textit{Test 5. } T_{31} > T_{31}^* + \mu_{31} - C_4.$$
$$(C_1 = 3.5, \; C_2 = 6.0, \; C_3 = 3.0, \; C_4 = 4.0).$$

After testing, some pixel is classified as the fire, providing the following conditions are fulfilled:

a) test 1 or (test 2 + test 3 + test 4 + test 5) for daytime pixels;

b) test 1 or (test 2 + test 3 + test 4) for nighttime pixels.

To increase the sensitivity of this algorithm in detection of HTOs with a relatively low intensity of the thermal emission, we have modified the MOD14 algorithm with:

a) considerably lowering the thresholds (5): $T_{21} > 302$ K (versus former 310 K) and $\Delta T > 3.5$ K (versus 10 K); and

b) changing the coefficients $C_1...C_4$ (6): $C_1 = 2.5$, $C_2 = 5.0$, $C_3 = 2.0$.

2.2. Description of the algorithm based on the RTM method

Stage 1. Based on the EOS/MODIS satellite telemetry, the IMAPP program is used to determine the *a priori* optical-meteorological information on the atmosphere state for regions of detecting high-temperature sources. The *a priori* information includes the following data:

− a spatial resolution of 1 km: the cloud mask (MOD35), the integrated atmospheric moisture content (MOD05);

− a spatial resolution of 5 km: vertical profiles of the geopotential, the air temperature, humidity, ozone content (MOD07), and cloud characteristics (MOD06);

− a spatial resolution of 10 km: aerosol optical characteristics (MOD04).

Emittances of the pixels ε_λ are determined by the standard method based on maps of surface types and tables of the correspondence of ε_λ to these Earth's surface types.

Stage 2. The cases of water pixels, as well as pixels, covered with thick clouds, are rejected with the use of MOD35, MOD06, and MOD05 data.

Stage 3. For channels 21/22 (henceforth, channel 21), 31, and 32, the *a priori* information, obtained earlier, is used to calculate the characteristics of the

thermal radiation distortion by the modified version of MODTRAN_v3.5 program. Then, based on the solution of thermal radiative transfer equation, $T_{S,21}$, $T_{S,31}$, and $T_{S,32}$ are calculated, i.e., LST values, retrieved in channels 21, 31, and 32. For correct temperature and humidity profiles in the absence of LST values, the condition of approximate equality $T_{S,21} \approx T_{S,31} \approx T_{S,32}$ is to be satisfied.

Stage 4. If $T_{S,31} \neq T_{S,32}$, then one of the reasons for this are errors in profiles of the meteorological parameters. In this case, the simplest compensation of these errors is conducted through calculating corrections of the form $\Delta T_S = C_{ERR}(T_{S,32} - T_{S,31})$ and of a new value of $T_{S,31} = T_{S,31} - \Delta T_S$.

Stage 5. In the case of influence of cirrus and semitransparent clouds, the retrieved LST values are corrected: $T_{S,21} = T_{S,21} + \Delta T_{21,CLD}$, $T_{S,31} = T_{S,31} + \Delta T_{31,CLD}$, where the "cloud" corrections are determined via *Look-Up-Table* of the influence of cloud characteristics on LST retrieval results and the mutual analysis of MOD35, MOD06, and MOD05 data.

Stage 6. The HTO detection is performed with the use of two conditions:

$$T_{S,21} > 302 \text{ K and } \Delta T = T_{S,21} - T_{S,31} > 3.5 \text{ K}.$$

2.3. Detection results

Table 4 presents the results of detection of test objects (torches) with the use of two (original and author-modified) MOD14 algorithms, as well as the RTM method for the temperature monitoring of the Earth surface, proposed by us. Table 4 gives results of torch detection, summed over all torches (N_Σ), the number of detections of each torch, and average temperature for each torch ($T_{21,av}$).

When testing the algorithm, totally 38 128 pixels in the torch neighborhood were processed. Note that the condition $T_{S,21} \approx T_{S,31} \approx T_{S,32}$ in the absence of clouds and HTOs does hold, signifying a good quality of the atmospheric correction of satellite LST measurements. For instance, for the sample, consisting of 30 985 pixels, corresponding to conditions of the clear-sky atmosphere, average retrieved LSTs were: $T_{S,21} = 298.4$ K, $T_{S,31} = 298.4$ K, $T_{S,32} = 298.7$ K. That is, the uncertainty in accounting for the molecular absorption in the EOS/MODIS channels 21/22, 31, and 32 was, on the average, less than 0.5 K.

The number of torch detections N_Σ with the use of the MOD14 v5.0.1 algorithm was 60, with identification of 6 test objects from 13. For the

MOD14_v5.0.1 algorithm, modified by us, (MOD14*), $N_\Sigma = 83$ at identified 10 test objects. With the use of the RTM method, N_Σ reached 122, and all 13 test objects were observed at a varying frequency.

Thus, the RTM method is on the average by a factor of two more efficient than the standard MOD14_v5.0.1 algorithm. In the modified algorithm version MOD14*, the detection thresholds of potential fires coincide with thresholds in the RTM method. However, in this case again the RTM method is far (almost by a factor of 1.5) more efficient than MOD14*.

Speaking about comparative estimates of the efficiency of these three algorithms, it is very important to note the following. Among test objects we can distinguish three bright torches (X1…X3, see Table 4), located in the south of the Tyumen Region, for which the detection frequency is markedly higher than for other torches at a less dependence on the choice of the method. Considering that the RTM method shows its main advantages in detection of relatively low-intensity thermal sources, it is advisable to obtain comparative estimates of application of the methods to such sources, namely, ten torches (F1…F10, see Table 4), located at the Tomsk Region. In this case, N_Σ ratio for three considered algorithms is already 6:21:53 for MOD14, MOD14*, and RTM, respectively, therefore, advantages of the RTM method markedly increase.

Let us compare the efficiency of application of the RTM method and the algorithm used at IAO SB RAS,[9] namely, the algorithm of the forest fire detection from data of the satellite system NOAA POES, when detecting low-intensity torches. In this case, the N_Σ ratio will be 36:53 for the IAO algorithm and the RTM method, respectively.

Thus, among the considered satellite methods, the RTM method, proposed by us, is the most efficient. Then the IAO algorithm follows and two variants of the MOD14 algorithm conclude the list.

Conclusion

The RTM method uses real-time satellite meteorological data on the atmospheric state at the moments of satellite observations and permits accounting for the distorting effect of the molecular atmosphere with an error less than 0.5 K. The use of the RTM method by the "*split-window*" principle makes this solution resistant to errors in setting the *a priori* meteorological information.

**Table 4. Results of detection of 13 test objects (torches) from space
with the help of three satellite methods**

Method	N_Σ	Torches												
		F1	F2	F3	F4	F5	F6	F7	F8	F9	F10	X1	X2	X3
MOD14	60	4	–	–	–	–	–	–	–	1	1	14	14	26
MOD14*	83	6	2	–	1	–	1	1	–	6	4	18	18	26
RTM	122	13	4	3	4	2	8	1	1	8	9	21	21	27
$T_{21,CP}$		309	304	306	306	305	305	308	303	307	306	314	320	329

In detection of high-temperature objects, the RTM method has considerable advantages over standard approaches, especially, for the problem of detection of low-intensity sources under complex optical-meteorological observation conditions.

References

1. F. Becker and Z.L. Li, Int. J. Remote Sens. **11**, No. 3, 369–393 (1990).
2. C. Ottle' and D. Vidal-Madjar, Remote Sens. Environ. **40**, No. 1, 27–41 (1992).
3. Z.L. Li and F. Becker, Remote Sens. Environ. **43**, No. 1, 67–85 (1993).
4. J.A. Sobrino, Z.L. Li, M.P. Stoll, and F. Becker, IEEE Trans. Geosci. and Remote Sens. **32**, No. 2, 243–253 (1994).
5. A.B. Uspenskii and G.I. Shcherbina, Issled. Zemli iz Kosmosa, No. 5, 102–112 (1996).
6. Z. Wan and J. Dozier, IEEE Trans. Geosci. and Remote Sens. **34**, No. 4, 892–905 (1996).
7. Z. Wan, MODIS Land-Surface Temperature Algorithm Theoretical Background Document (LST ATBD), version 3.3 Inst. for Comput. Earth Syst. Sci., Univ. of Calif., Santa Barbara (1999). Electronic resource: http://modis. gsfc.nasa.gov/data/atbd/atbd_mod11.pdf
8. K. Mao, Z. Qin, J. Shi, and P. Gong, Int. J. Remote Sens. **15**, No. 15, 3181–3204 (2005).
9. V.V. Belov and S.V. Afonin, *From Physical Foundations, Theory, and Simulation to Thematic Processing of Satellite Images* (Publishing House of IAO SB RAS, 2005), 266 pp.
10. K. Thome, F. Palluconi, T. Takashima, and K. Masuda, IEEE Trans. Geosci. and Remote Sens. **36(4)**, 1199–1211 (1998).
11. J.A. Sobrino, J.C. Jiménez-Muñoz, and L. Paolini, Remote Sens. Environ. **90**, No. 4, 434–440 (2004).
12. S.V. Afonin and D.V. Solomatov, Atmos. Oceanic Opt. **21**, No. 2, 125–131 (2008).
13. P. Wang, Y.L. Karen, T. Cwik, and R. Green, Parallel Computing **28**, Is. 1, 53–64 (2002).
14. V.A. Golovko, Issled. Zemli iz Kosmosa, No. 2, 11–23 (2006).
15. S.A. Clough, M.W. Shephard, E.J. Mlawer, J.S. Delamere, M.J. Iacono, K. Cady-Pereira, S. Boukabara, and P.D. Brown, J. Quant. Spectrosc. and Radiat. Transfer **91**, No. 2, 233–244 (2005).
16. L.S. Rothman, D. Jacquemart, A. Barbe, D.C. Benner, M. Birk, L.R. Brown, M.R. Carleer, C. Chackerian, Jr., K. Chance, V. Dana, V.M. Devi, J.-M. Flaud, R.R. Gamache, A. Goldman, J.-M. Hartmann, K.W. Jucks, A.G. Maki, J.-Y. Mandin, S.T. Massie, J. Orphal, A. Perrin, C.P. Rinsland, M.A.H. Smith, J. Tennyson, R.N. Tolchenov, R.A. Toth, J. Auwera Vander, P. Varanasi, and G. Wagner, J. Quant. Spectrosc. and Radiat. Transfer **96**, No. 2, 139–204 (2005).
17. M.J. Mlawer, D.C. Tobin, and S.A. Clough, J. Quant. Spectrosc. and Radiat. Transfer (2004) (in press).
18. F.X. Kneizys, L.W. Abreu, G.P. Anderson, J.H. Chetwynd, E.P. Shettle, A. Berk, L.S. Bernstein, D.C. Robertson, P. Acharya, L.S. Rothman, J.E.A. Selby, W.O. Gallery, and S.A. Clough, *The MODTRAN 2/3 Report and LOWTRAN 7 Model*, Phillips Laboratory, Hanscom AFB contract F19628-91-C-0132 with Ontar Corp. (1996).
19. A. Berk, G. Anderson, P. Acharya, M. Hoke, J. Chetwynd, L. Bernstein, E. Shettle, M. Matthew, and S. Adler-Golden, MODTRAN4 Version 3 Revision 1 User's Manual, Air Force Res. Lab., Hanscom Air Force Base, Mass (2003).
20. L.S. Rothman, C.P. Rinsland, A. Goldman, S.T. Massie, D.P. Edwards, J.-M. Flaud, A. Perrin, C. Camy-Peyret, V. Dana, J.Y. Mandin, J. Schröder, A. McCann, R.R. Gamache, R.B. Wattson, K. Yoshino, K.V. Chance, K.W. Jucks, L.R. Brown, V. Nemtchinov, and P. Varanasi, J. Quant. Spectrosc. and Radiat. Transfer **60**, No. 5, 665–710 (1998).
21. S.A. Clough, F.X. Kneizys, and R.W. Davies, Atmos. Res. **23**, Nos. 3–4, 229–241 (1989).
22. S.W. Seemann, J. Li, W.P. Menzel, and L.E. Gumley, J. Appl. Meteorol. **42**, No. 8, 1072–1091 (2003).
23. L. Giglio, J. Descloitres, C.O. Justice, and Y.J. Kaufman, Remote Sens. Environ. **83**, Nos. 2–3, 273–282 (2003).